2008 IEEE International Conference on
Robotics and Automation
Pasadena, CA, USA, May 19-23, 2008

An IMC Based Enhancement of Accuracy and Robustness of Impedance Control

Sang Hoon Kang, Maolin Jin, and Pyung Hun Chang, *Member, IEEE*

Abstract— **An accurate and robust impedance control technique is developed based on internal model control structure and time–delay estimation: the former injects desired impedance and corrects dynamics estimation error; the latter estimates and compensates the nonlinear dynamics of robot manipulators. Owing to the simple structure, the proposed control is designed without requiring entire dynamics computation or complex algorithms. The accuracy and robustness of the proposed control are verified using a two degrees of freedom robot with stiff wall simulation. The proposed control realizes desired impedance accurately compared with other competent controllers throughout the task, i.e., free motion, constrained motion, and transition between these motions. Further, proposed control realizes four sets of desired impedance accurately. Thus, accuracy and robustness of proposed control is confirmed.**

I. Introduction

For more than two decades since it was first reported, impedance control has been noted and recognized as a promising unified approach to robot manipulation [1]. Thus, it has been applied to many robotic systems.

Recently, however, it was revealed in [2] that it is difficult to enhance robustness against modeling error without losing the accuracy at which the desired impedance is attained. This is known as the "Accuracy/Robustness Dilemma in Impedance Control" [2]. In short, the N. Hogan's original method [1], called DB-IC (Dynamics Based Impedance Control) [2], compensates robot dynamics by using a dynamic model [2]. Thus, DB-IC is sensitive to modeling error. In contrast, Position Based Impedance Control (PB-IC), one of the most common implementation of impedance control [2]-[8], can enhance robustness against modeling error using an inner loop [2], [4]-[8]. However, because of the modeling error, the inner loop dynamics, expected to be hidden, is excited and degrades impedance realization accuracy [2].

As a trade-off between accuracy and robustness, Instantaneous Model based Impedance Control (IM-IC) was proposed in [2]. However, in this case as well, accuracy is degraded because of inner loop dynamics [2].

This work was supported by the Korea Science and Engineering Foundation (KOSEF) grant funded by the Korea government (MOST) (No. R01-2006-000-10872-0).

The authors are with the Robotics and Control Laboratory, Department of Mechanical Engineering, KAIST, 305-701, Daejeon, Republic of Korea (phone: 82-42-869-3266; fax: 82-42-869-5226; e-mail: shkang@mecha.kaist.ac.kr).

Many research works have been carried out with the aim of attaining robustness of impedance control. Notable approaches include variable structure control [9], adaptive control [10], and iterative learning control [11]. Although these approaches succeeded to enhance robustness, they use either a computationally demanding robot dynamics model or complex algorithms. Therefore, in addition to accuracy and robustness, simplicity of the control law is preferable.

With these considerations in mind, in response to the given dilemma, an Internal Model Control (IMC) [12] based impedance control was developed. IMC was chosen to inject desired impedance dynamics while correcting modeling error by using so-called *perfect control* performance. To reduce the use of dynamics model of proposed control, Time Delay Estimation (TDE) [13], a *model-independent* dynamics estimation technique [13]-[16], was incorporated. Simulation results verify the accuracy and robustness of proposed control law in comparison with other control laws.

This paper is structured as follows. Section II briefly introduces DB-IC, PB-IC, and the "Accuracy /Robustness Dilemma". In Section III, an impedance control scheme is proposed and analyzed. Section IV presents a comparison of the proposed approach, the DB-IC, the PB-IC, and the IM-IC through two DOF simulations. Also the impedance realization accuracy of proposed control is verified using four sets of desired impedance. Finally, in Section V, we summarize the results and draw conclusions.

II. Accuracy/Robustness Dilemma

A. Desired Impedance

The goal of impedance control [4]-[8] is to achieve desired impedance dynamics as follows:

$$\mathbf{M}_d(\ddot{\mathbf{x}}_d - \ddot{\mathbf{x}}) + \mathbf{B}_d(\dot{\mathbf{x}}_d - \dot{\mathbf{x}}) + \mathbf{K}_d(\mathbf{x}_d - \mathbf{x}) = \mathbf{F}_e, \quad (1)$$

where $\mathbf{x}, \dot{\mathbf{x}}, \ddot{\mathbf{x}} \in \Re^n$ denote the Cartesian position, and its time derivatives, respectively; $\mathbf{x}_d, \dot{\mathbf{x}}_d, \ddot{\mathbf{x}}_d \in \Re^n$ denote the Cartesian desired trajectory and its time derivatives, respectively; $\mathbf{F}_e \in \Re^n$ the interaction force on the environment exerted by the robot; and $\mathbf{M}_d, \mathbf{B}_d, \mathbf{K}_d \in \Re^{n\times n}$ denote the desired mass, damping, and stiffness, respectively. In the Laplace domain, $\mathbf{Z}_d(s) \in \Re^{n\times n}$, a desired dynamic relation between $\mathbf{F}_e$ and $\mathbf{x}$, has the following form:

$$\mathbf{Z}_d(s) = s^2\mathbf{M}_d + s\mathbf{B}_d + \mathbf{K}_d. \quad (2)$$

$\mathbf{Z}_d$ is, in general, selected not for the enhancement of robustness, but for achievement of the task objective [1].

B. Robot Dynamics

For the Cartesian space control, usually two forms of robot dynamics are considered [2], [17]: one form [2] is

$$\boldsymbol{\tau}_u = \mathbf{M}_\theta(\boldsymbol{\theta})\mathbf{J}^{-1}(\boldsymbol{\theta})(\ddot{\mathbf{x}} - \dot{\mathbf{J}}\dot{\boldsymbol{\theta}}) + \mathbf{N}_\theta(\boldsymbol{\theta},\dot{\boldsymbol{\theta}}) + \mathbf{J}^T(\boldsymbol{\theta})\mathbf{F}_e \,. \quad (3)$$

where $\boldsymbol{\theta},\dot{\boldsymbol{\theta}} \in \Re^n$ denote the joint position and velocity, respectively; $\mathbf{M}_\theta(\boldsymbol{\theta}) \in \Re^{n\times n}$ the inertia matrix; $\mathbf{N}_\theta(\boldsymbol{\theta},\dot{\boldsymbol{\theta}}) \in \Re^n$ the centrifugal, Coriolis, gravitational, and friction forces; $\mathbf{J}(\boldsymbol{\theta}) \in \Re^{n\times n}$ the Jacobian; and $\boldsymbol{\tau}_u \in \Re^n$ the input torque.

The other form [17] is an operational space formulation of robot dynamics.

$$\mathbf{F}_u = \mathbf{M}_x(\boldsymbol{\theta})\ddot{\mathbf{x}} + \mathbf{N}_x(\boldsymbol{\theta},\dot{\boldsymbol{\theta}}) + \mathbf{F}_e \,, \quad (4)$$

where $\mathbf{M}_x = \mathbf{J}^{-T}\mathbf{M}_\theta\mathbf{J}^{-1}$, and $\mathbf{N}_x = \mathbf{J}^{-T}[\mathbf{N}_\theta - \mathbf{M}_\theta\mathbf{J}^{-1}\dot{\mathbf{J}}\dot{\boldsymbol{\theta}}]$.

C. Dynamics Based Impedance Control (DB-IC)

Based on (3), the following DB-IC law is derived [1], [4].

$$\boldsymbol{\tau}_u = \hat{\mathbf{M}}_\theta(\boldsymbol{\theta})\mathbf{J}^{-1}(\boldsymbol{\theta})(\mathbf{u}_d - \dot{\mathbf{J}}\dot{\boldsymbol{\theta}}) + \hat{\mathbf{N}}_\theta(\boldsymbol{\theta},\dot{\boldsymbol{\theta}}) + \mathbf{J}^T(\boldsymbol{\theta})\mathbf{F}_e \text{ with} \quad (5)$$

$$\mathbf{u}_d = \ddot{\mathbf{x}}_d + \mathbf{M}_d^{-1}[\mathbf{B}_d(\dot{\mathbf{x}}_d - \dot{\mathbf{x}}) + \mathbf{K}_d(\mathbf{x}_d - \mathbf{x}) - \mathbf{F}_e] \,, \quad (6)$$

where $\hat{\mathbf{M}}_\theta(\boldsymbol{\theta}) \in \Re^{n\times n}$ and $\hat{\mathbf{N}}_\theta(\boldsymbol{\theta},\dot{\boldsymbol{\theta}}) \in \Re^n$ denote estimates of $\mathbf{M}_\theta$ and $\mathbf{N}_\theta$, respectively; and $\mathbf{u}_d \in \Re^n$ denotes the control input. In the Laplace domain, $\mathbf{u}_d$ can be written as below:

$$\mathbf{u}_d = \mathbf{M}_d^{-1}\mathbf{Z}_d(s)\mathbf{x}_d - \mathbf{M}_d^{-1}\mathbf{F}_e - \mathbf{M}_d^{-1}(s\mathbf{B}_d + \mathbf{K}_d)\mathbf{x} \,. \quad (7)$$

Clearly, robustness of the DB-IC entirely relies on the estimated values, $\hat{\mathbf{M}}_\theta$ and $\hat{\mathbf{N}}_\theta$.

D. Position Based Impedance Control (PB-IC)

PB-IC works as follows. The desired impedance model modifies $\mathbf{x}_d$ by using $\mathbf{F}_e$. The modified trajectory is then imposed as a command of the inner position control loop [2], [4]-[8]. The position command of the inner loop is the solution to the following desired impedance model:

$$\mathbf{M}_d(\ddot{\mathbf{x}}_d - \ddot{\mathbf{x}}_r) + \mathbf{B}_d(\dot{\mathbf{x}}_d - \dot{\mathbf{x}}_r) + \mathbf{K}_d(\mathbf{x}_d - \mathbf{x}_r) = \mathbf{F}_e \,, \quad (8)$$

where $\mathbf{x}_r, \dot{\mathbf{x}}_r, \ddot{\mathbf{x}}_r \in \Re^n$ denote the inner loop position command and its time derivatives, respectively. In the Laplace domain, $\mathbf{x}_r$ can be obtained as follows:

$$\mathbf{x}_r = \mathbf{Z}_d^{-1}(s)\mathbf{M}_d[\mathbf{M}_d^{-1}\mathbf{Z}_d(s)\mathbf{x}_d - \mathbf{M}_d^{-1}\mathbf{F}_e] = \mathbf{x}_d - \mathbf{Z}_d^{-1}(s)\mathbf{F}_e \,. \quad (9)$$

If the inner loop guarantees zero position error ($\mathbf{x}=\mathbf{x}_r$), then, from (8), desired impedance is attained [5]. In free space, small $\mathbf{x}_r-\mathbf{x}$ implies small position error, because $\mathbf{x}_r=\mathbf{x}_d$ [5]. Thus, close following of $\mathbf{x}_r$ means i) small impedance error in constrained space and ii) small position error in free space.

Any position control can be used for the inner loop. In this study, an experimentally verified method in [4], [8] is selected. It also uses the same dynamics compensation of (5). The difference is that $\mathbf{u}_d$ is replaced with $\mathbf{u}_p$:

$$\mathbf{u}_p = \ddot{\mathbf{x}}_r + \mathbf{K}_v(\dot{\mathbf{x}}_r - \dot{\mathbf{x}}) + \mathbf{K}_p(\mathbf{x}_r - \mathbf{x}) \,, \quad (10)$$

where $\mathbf{K}_p, \mathbf{K}_v \in \Re^{n\times n}$ denote inner loop gains which can be designed independently of $\mathbf{M}_d$, $\mathbf{B}_d$, and $\mathbf{K}_d$.

E. Accuracy/Robustness Dilemma in Impedance Control

The robot dynamics (3) can be rewritten as follows:

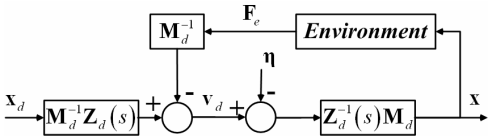

Fig.1 Block diagram of the DB-IC

$$\begin{aligned}\boldsymbol{\tau}_u = {} & \hat{\mathbf{M}}_\theta\mathbf{J}^{-1}(\ddot{\mathbf{x}} - \dot{\mathbf{J}}\dot{\boldsymbol{\theta}}) + \hat{\mathbf{N}}_\theta + \mathbf{J}^T\mathbf{F}_e \\ & + (\mathbf{M}_\theta - \hat{\mathbf{M}}_\theta)\mathbf{J}^{-1}(\ddot{\mathbf{x}} - \dot{\mathbf{J}}\dot{\boldsymbol{\theta}}) + (\mathbf{N}_\theta - \hat{\mathbf{N}}_\theta)\end{aligned} \,. \quad (11)$$

Subtracting (11) from (5) yields

$$\hat{\mathbf{M}}_\theta\mathbf{J}^{-1}(\mathbf{u} - \ddot{\mathbf{x}}) = (\mathbf{M}_\theta - \hat{\mathbf{M}}_\theta)\mathbf{J}^{-1}(\ddot{\mathbf{x}} - \dot{\mathbf{J}}\dot{\boldsymbol{\theta}}) + (\mathbf{N}_\theta - \hat{\mathbf{N}}_\theta) \,. \quad (12)$$

Now, we define the *dynamics estimation error*, $\boldsymbol{\eta}_{(t)} \in \Re^n$:

$$\boldsymbol{\eta}_{(t)} \triangleq \mathbf{J}\hat{\mathbf{M}}_\theta^{-1}[(\mathbf{M}_\theta - \hat{\mathbf{M}}_\theta)\mathbf{J}^{-1}(\ddot{\mathbf{x}} - \dot{\mathbf{J}}\dot{\boldsymbol{\theta}}) + (\mathbf{N}_\theta - \hat{\mathbf{N}}_\theta)] = \mathbf{u}_{(t)} - \ddot{\mathbf{x}}_{(t)} \quad (13)$$

$\mathbf{u}$ has no subscript, because (12) is a common relation to both DB-IC and PB-IC. $\mathbf{u}$ and $\mathbf{x}$ have a linear 2nd order dynamics, subject to $\boldsymbol{\eta}$.

$$\mathbf{u} = s^2\mathbf{x} + \boldsymbol{\eta} \,. \quad (14)$$

1) Accuracy and Robustness of the DB-IC

$\mathbf{u}_d$ can be divided into two parts as follows:

$$\mathbf{u}_d = \mathbf{v}_d - \mathbf{M}_d^{-1}(s\mathbf{B}_d + \mathbf{K}_d)\mathbf{x} \quad (15)$$

where $\mathbf{v}_d \triangleq \mathbf{M}_d^{-1}\mathbf{Z}_d(s)\mathbf{x}_d - \mathbf{M}_d^{-1}\mathbf{F}_e$. Substituting (15) into (14), and solving for $\mathbf{x}$, we have

$$\mathbf{x} = \mathbf{Z}_d^{-1}(s)\mathbf{M}_d[\mathbf{v}_d - \boldsymbol{\eta}] \,, \quad (16)$$

which is illustrated in Fig.1. From (9) and the definition of $\mathbf{v}_d$, $\mathbf{v}_d$ can be rewritten as follows:

$$\mathbf{v}_d = \mathbf{M}_d^{-1}\mathbf{Z}_d(s)\mathbf{x}_r \,. \quad (17)$$

Note that DB-IC does not use $\mathbf{x}_r$. $\mathbf{x}_r$ is introduced to compare DB-IC with other control laws in a consistent manner. Substituting (17) into (16) and solving for $\mathbf{x}_r-\mathbf{x}$, we have

$$\mathbf{x}_r - \mathbf{x} = \mathbf{Z}_d^{-1}(s)\mathbf{M}_d\boldsymbol{\eta} = (s^2\mathbf{I} + s\mathbf{M}_d^{-1}\mathbf{B}_d + \mathbf{M}_d^{-1}\mathbf{K}_d)^{-1}\boldsymbol{\eta} \,. \quad (18)$$

Accurate realization of desired impedance is disturbed by $\boldsymbol{\eta}$. Moreover, except $\mathbf{M}_d$, $\mathbf{B}_d$, and $\mathbf{K}_d$, there are no other gains to suppress the effect of $\boldsymbol{\eta}$. Thus, DB-IC is sensitive to $\boldsymbol{\eta}$.

2) Accuracy and Robustness of the PB-IC

Similar to (15), $\mathbf{u}_p$ can be divided into two parts as follows:

$$\mathbf{u}_p = \mathbf{v}_p - (s\mathbf{K}_v + \mathbf{K}_p)\mathbf{x} \quad (19)$$

where $\mathbf{v}_p \triangleq \mathbf{C}(s)\mathbf{x}_r$; and $\mathbf{C}(s) \triangleq s^2\mathbf{I} + s\mathbf{K}_v + \mathbf{K}_p$. Substituting (19) into (14), and solving for $\mathbf{x}$, we have

$$\mathbf{x} = \mathbf{C}^{-1}(s)(\mathbf{v}_p - \boldsymbol{\eta}) \,. \quad (20)$$

The relations, (9) and (20), are illustrated in Fig.2. By substituting the definition of $\mathbf{v}_p$ into (20) and solving for $\mathbf{x}_r-\mathbf{x}$, we have

$$\mathbf{x}_r - \mathbf{x} = \mathbf{C}^{-1}(s)\boldsymbol{\eta} = (s^2\mathbf{I} + s\mathbf{K}_v + \mathbf{K}_p)^{-1}\boldsymbol{\eta} \,. \quad (21)$$

$\mathbf{C}^{-1}(s)$ can attenuate the effect of $\boldsymbol{\eta}$ by increasing $\mathbf{K}_p$, $\mathbf{K}_v$. Thus, PB-IC has better robustness compared with that of DB-IC.

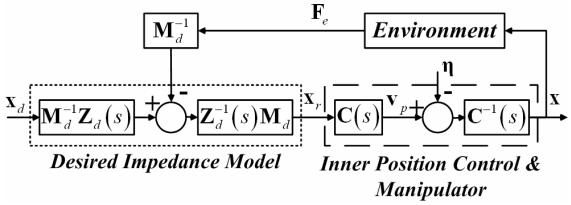

Fig. 2. Block diagram of the PB-IC

However, it is clear from Fig.2 that inner loop dynamics $\mathbf{C}^{-1}(s)$, meant to be canceled by $\mathbf{C}(s)$, is excited by $\boldsymbol{\eta}$ and hinders accurate realization of the desired impedance. Thus, the inaccuracy is related to the inner loop dynamics. In the worst case, the robot can lose contact and oscillates [2].

3) Accuracy/Robustness Dilemma

Although DB-IC can realize desired impedance accurately with precise model, it is sensitive to the modeling error. Although PB-IC can enhance robustness against the modeling error, it realizes inaccurate impedance because of the inherent inner loop dynamics, which is, in general, different from the desired impedance dynamics. Thus, there is a dilemma between accuracy and robustness.

Remark: As a trade-off solution, IM-IC was developed in [2]. However, it also uses inner loop. Thus, IM-IC has the accuracy problem, too.

III. Proposed Impedance Control

A brief review of IMC and TDE is presented. The proposed control law is then derived and analyzed.

A. Internal Model Control

The closed-loop dynamics due to IMC (Fig.3) is given as:

$$y=\{(PQ)/[1+(P-\tilde{P})Q]\}y_d+\{(1-\tilde{P}Q)/[1+(P-\tilde{P})Q]\}Pd. \quad (22)$$

From (22), one can easily derive the *perfect control* property of IMC [12]: assuming that $Q=\tilde{P}^{-1}$, and the closed-loop is stable, then *perfect control* ($y=y_d$) is achieved. It is proved in [12]. This condition only restricts the relation between Q and $\tilde{P}$, not the plant P. Further, the design is straightforward: $\tilde{P}$ is set to be the same as the plant model, and $Q=\tilde{P}^{-1}$ [12].

However, as many other controllers, IMC also requires robot dynamics model. This could be resolved by using TDE.

B. Time Delay Estimation

TDE works as follows [13]. The dynamics of (4) can be divided into two terms, the known term and the unknown and uncertain nonlinear terms, $\mathbf{H}(\boldsymbol{\theta},\mathbf{x},\dot{\mathbf{x}},\ddot{\mathbf{x}})\in\Re^n$, as follows:

$$\mathbf{F}_u=\bar{\mathbf{M}}_x\ddot{\mathbf{x}}+\mathbf{H}(\boldsymbol{\theta},\mathbf{x},\dot{\mathbf{x}},\ddot{\mathbf{x}}), \quad (23)$$

where $\bar{\mathbf{M}}_x\in\Re^{n\times n}$ denotes the known part of $\mathbf{M}_x$, and $\mathbf{H}(\boldsymbol{\theta},\mathbf{x},\dot{\mathbf{x}},\ddot{\mathbf{x}})\triangleq[\mathbf{M}_x(\boldsymbol{\theta})-\bar{\mathbf{M}}_x]\ddot{\mathbf{x}}+\mathbf{N}_x(\boldsymbol{\theta},\dot{\boldsymbol{\theta}})+\mathbf{F}_e$. Then, for a sufficiently small time delay L, $\hat{\mathbf{H}}_{(t)}$, the time delayed estimate of $\mathbf{H}_{(t)}$, can be obtained as below [13]:

$$\hat{\mathbf{H}}_{(t)}=\mathbf{H}_{(t-L)}=\mathbf{F}_{u(t-L)}-\bar{\mathbf{M}}_x\ddot{\mathbf{x}}_{(t-L)}. \quad (24)$$

Mostly, L is the sampling time in digital implementation.

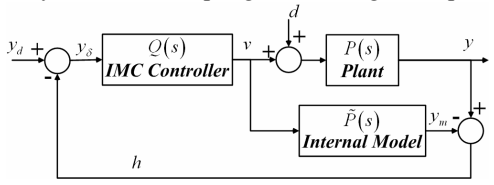

Fig. 3. Block diagram of the IMC, where Q denotes the IMC controller, P signifies the plant, and $\tilde{P}$ denotes the internal model.

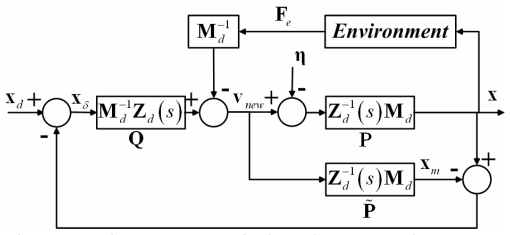

Fig.4. The proposed IMC structure for impedance control.

TDE does not require a dynamic model or parameters. It only needs the recent past information of acceleration and input force[1]. Similar to the definition of $\boldsymbol{\eta}$, TDE error, $\boldsymbol{\eta}_{T(t)}\in\Re^n$, is defined as follows:

$$\boldsymbol{\eta}_{T(t)}\triangleq\bar{\mathbf{M}}_x^{-1}[\mathbf{H}_{(t)}-\hat{\mathbf{H}}_{(t)}]. \quad (25)$$

Note that TDE error is also a dynamics estimation error.

TDE is applied to the proposed control to remove the need of an entire robot dynamic model.

C. Derivation of the Proposed Impedance Control Law

1) IMC Structure for Impedance Control

In comparison with the structure of IMC (Fig.3), we found that the closed-loop due to DB-IC (Fig.1) is an IMC applicable form: the feed forward controller $\mathbf{M}_d^{-1}\mathbf{Z}_d$ and the plant $\mathbf{Z}_d^{-1}\mathbf{M}_d$, with $\boldsymbol{\eta}$ acting as an input disturbance to the plant. The only difference is that $\mathbf{F}_e$ is separated from $\boldsymbol{\eta}$ for impedance control. Thus, the *perfect control* property of IMC should be able to improve the robustness against modeling error, and the impedance accuracy regardless of environment stiffness – this is the *key concept* of this paper.

By following the standard IMC design procedure, an internal model loop is added to the closed-loop in Fig.1. The IMC controller $\mathbf{Q}=\mathbf{M}_d^{-1}\mathbf{Z}_d(s)$ is already given in Fig 1. The internal model $\tilde{\mathbf{P}}$ is simply selected as follows:

$$\tilde{\mathbf{P}}=\mathbf{Z}_d^{-1}(s)\mathbf{M}_d. \quad (26)$$

Adding IMC feedback, the proposed control is achieved (Fig. 4). The input to $\mathbf{Q}$ is changed from $\mathbf{x}_d$ to $\mathbf{x}_\delta$, and thus $\mathbf{u}_d$ and $\mathbf{v}_d$ are replaced with $\mathbf{u}_{new}$ and $\mathbf{v}_{new}$ as follows:

$$\mathbf{u}_{new(t)}=\mathbf{v}_{new(t)}-\mathbf{M}_d^{-1}\left(\mathbf{B}_d\dot{\mathbf{x}}_{(t)}+\mathbf{K}_d\mathbf{x}_{(t)}\right), \quad (27)$$

$$\mathbf{v}_{new(t)}=\mathbf{M}_d^{-1}\left(\ddot{\mathbf{x}}_{\delta(t)}+\mathbf{B}_d\dot{\mathbf{x}}_{\delta(t)}+\mathbf{K}_d\mathbf{x}_{\delta(t)}\right)-\mathbf{M}_d^{-1}\mathbf{F}_{e(t)}. \quad (28)$$

From Fig.4, one can directly deduce the following relations:

$$\mathbf{x}=\mathbf{Z}_d^{-1}(s)\mathbf{M}_d(\mathbf{v}_{new}-\boldsymbol{\eta}). \quad (29)$$

$$\begin{aligned}\mathbf{x}-\mathbf{x}_m&=\mathbf{Z}_d^{-1}(s)\mathbf{M}_d(\mathbf{v}_{new}-\boldsymbol{\eta})-\mathbf{Z}_d^{-1}(s)\mathbf{M}_d\mathbf{v}_{new},\\&=-\mathbf{Z}_d^{-1}(s)\mathbf{M}_d\boldsymbol{\eta}\end{aligned} \quad (30)$$

$$\begin{aligned}\mathbf{v}_{new}&=\mathbf{M}_d^{-1}\mathbf{Z}_d(s)\mathbf{x}_\delta-\mathbf{M}_d^{-1}\mathbf{F}_e\\&=\mathbf{M}_d^{-1}\mathbf{Z}_d(s)[\mathbf{x}_d-(\mathbf{x}-\mathbf{x}_m)]-\mathbf{M}_d^{-1}\mathbf{F}_e\\&=\mathbf{v}_d+\underbrace{\boldsymbol{\eta}}_{\text{correcting dynamics estimation error}}\end{aligned}. \quad (31)$$

From (30), the additional IMC feedback term $\mathbf{x}-\mathbf{x}_m$ is a function of $\boldsymbol{\eta}$ only. Thus, as shown in (31), the IMC feedback

[1] If only $\mathbf{x}$ is available, one can estimate one step delayed acceleration using up to two step delayed $\mathbf{x}$ as follows: $\ddot{\mathbf{x}}_{(t-L)}=(\mathbf{x}_{(t)}-2\mathbf{x}_{(t-L)}+\mathbf{x}_{(t-2L)})/L^2$.

term corrects dynamics estimation error. Substituting (17) and (31) into (29), and solving for $\mathbf{x}_r - \mathbf{x}$, we have

$$\mathbf{x}_r - \mathbf{x} = \mathbf{0}_n, \tag{32}$$

where $\mathbf{0}_n \in \Re^n$ denotes zero vector. Desired impedance is perfectly realized regardless of $\boldsymbol{\eta}$. In this sense, the proposed IMC structure is a perfect solution to the dilemma. In addition, the design is straightforward. Further, this structure requires only the desired impedance parameters. From (31), this structure requires acceleration, which might be noisy. The noise problem will be discussed in section III.E.1).

Because this structure requires computation of the entire robot dynamics as many other control laws, the simplicity factor needs to be improved.

2) Combining IMC structure with TDE

For simplicity, the complex model-based compensation (5) is replaced with TDE. From (23) and (24), the following dynamics compensation is obtained [13]:

$$\begin{cases} \mathbf{F}_{u(t)} = \bar{\mathbf{M}}_x \mathbf{u}_{new(t)} + \mathbf{F}_{u(t-L)} - \bar{\mathbf{M}}_x \ddot{\mathbf{x}}_{(t-L)} \\ \boldsymbol{\tau}_{u(t)} = \mathbf{J}^T \mathbf{F}_{u(t)} \end{cases}, \tag{33}$$

Thus, proposed control law consists of (27), (28), (33). Subtraction of (23) from (33), and a simple mathematical manipulation, yields

$$\mathbf{u}_{new(t)} - \ddot{\mathbf{x}}_{(t)} = \bar{\mathbf{M}}_x^{-1}[\mathbf{H}_{(t)} - \hat{\mathbf{H}}_{(t)}] = \boldsymbol{\eta}_{T(t)}. \tag{34}$$

Thus, (34) becomes

$$\mathbf{u}_{new} = s^2 \mathbf{x} + \boldsymbol{\eta}_T. \tag{35}$$

In comparison with (14), the only difference is that $\boldsymbol{\eta}$ is replaced by $\boldsymbol{\eta}_T$. Again, $\boldsymbol{\eta}_T$ can be regarded as a dynamics estimation error, which can be corrected by the proposed IMC structure.

Probably, proposed control will be implemented in discrete time domain. Thus, unavoidable feedback time delay is explicitly included in IMC feedback as below (see $\mathbf{x}_{(t-L)}$ and $\mathbf{x}_{m(t-L)}$):

$$\mathbf{x}_{\delta(t)} = \mathbf{x}_{d(t)} - \mathbf{x}_{(t-L)} + \mathbf{x}_{m(t-L)}. \tag{36}$$

Discrete implementation of proposed control will be considered in following sections for more realistic analysis.

D. Discussion of the Proposed Impedance Control Law

1) Accuracy and Robustness

Substituting (28) and (36) into (27), and subtracting (6) give the control input of the proposed control as follows:

$$\begin{aligned} \mathbf{u}_{new(t)} = \mathbf{u}_{d(t)} - \{ & (\ddot{\mathbf{x}}_{(t-L)} - \ddot{\mathbf{x}}_{m(t-L)}) \\ & + \mathbf{M}_d^{-1}[\mathbf{B}_d(\dot{\mathbf{x}}_{(t-L)} - \dot{\mathbf{x}}_{m(t-L)}) + \mathbf{K}_d(\mathbf{x}_{(t-L)} - \mathbf{x}_{m(t-L)})]\} \end{aligned}. \tag{37}$$

In the Laplace domain, (37) becomes

$$\mathbf{u}_{new} = \mathbf{u}_d - \mathbf{M}_d^{-1}\mathbf{Z}_d(s)e^{-Ls}(\mathbf{x} - \mathbf{x}_m). \tag{38}$$

Similar to the derivation of (30), in this case, $\mathbf{x}$-$\mathbf{x}_m$ becomes

$$\mathbf{x} - \mathbf{x}_m = -\mathbf{Z}_d^{-1}(s)\mathbf{M}_d\boldsymbol{\eta}_T. \tag{39}$$

The only difference between (30) and (39) is that $\boldsymbol{\eta}$ is replaced with $\boldsymbol{\eta}_T$. Substituting (7), (38), and (39) into (35), and solving for $\mathbf{x}_r - \mathbf{x}$, we have

$$\begin{aligned} \mathbf{x}_r - \mathbf{x} &= \mathbf{Z}_d^{-1}(s)\mathbf{M}_d(1 - e^{-Ls})\boldsymbol{\eta}_T \\ &= (s^2\mathbf{I} + s\mathbf{M}_d^{-1}\mathbf{B}_d + \mathbf{M}_d^{-1}\mathbf{K}_d)^{-1}(1 - e^{-Ls})\boldsymbol{\eta}_T \end{aligned}. \tag{40}$$

In comparison with (18) and (21), the dynamics estimation error (in this case, TDE error $\boldsymbol{\eta}_{T(t)}$) is corrected by a step delayed term $\boldsymbol{\eta}_{T(t-L)}$ without introducing any other dynamics such as $\mathbf{C}(s)$ of the PB-IC. Further, if the IMC feedback has no time delay, $\mathbf{x}$ becomes identical to $\mathbf{x}_r$, i.e., desired impedance dynamics can be perfectly realized.

In short, proposed control enhances robustness without introducing the problematic inner loop dynamics. Thus, it can be a solution to the dilemma.

2) The simplicity

The IMC loop requires no other gains except $\mathbf{M}_d$, $\mathbf{B}_d$, and $\mathbf{K}_d$, and can be designed in a straightforward manner. The TDE needs one gain, $\bar{\mathbf{M}}_x$, and only one step delayed acceleration and input force instead of computation of complex nonlinear dynamics such as Coriolis and centrifugal force, gravity, and friction force, thus providing a simple approach. Overall, the proposed control fully shares the advantages of IMC and TDE.

E. Practical Consideration

1) Noise Attenuation using Low Pass Filter

If digital 1st order low pass filter with the cut-off frequency λ is applied to reduce noise, (33) is changes as below [13]:

$$\mathbf{F}^*_{u(t)} = \bar{\mathbf{M}}_x \mathbf{u}_{new(t)} + \mathbf{F}_{u(t-L)} - \bar{\mathbf{M}}_x \ddot{\mathbf{x}}_{(t-L)} \tag{41}$$

$$\mathbf{F}_{u(t)} = [\lambda'/(1+\lambda')]\mathbf{F}^*_{u(t)} + [1/(1+\lambda')]\mathbf{F}_{u(t-L)} \quad (\lambda' = \lambda L) \tag{42}$$

where $\mathbf{F}^*_u$ denotes input to the filter. Substituting (42) into (41) leads to the following:

$$\mathbf{F}_{u(t)} = [\lambda'/(1+\lambda')]\bar{\mathbf{M}}_x \mathbf{u}_{new(t)} + \mathbf{F}_{u(t-L)} - [\lambda'/(1+\lambda')]\bar{\mathbf{M}}_x \ddot{\mathbf{x}}_{(t-L)}. \tag{43}$$

Thus, the use of a low pass filter has the same effect as lowering $\bar{\mathbf{M}}_x$. Note that no additional dynamics was introduced even with a low pass filter.

2) Removal of Internal Model Computation

To prevent numerical errors in computing $\mathbf{x}_m$, and to enhance simplicity of proposed control, (28) and (36) is modified. Substituting (36) into (28) yields

$$\mathbf{v}_{new} = \mathbf{M}_d^{-1}[\mathbf{Z}_d\mathbf{x}_d - \mathbf{F}_e] - \mathbf{M}_d^{-1}\mathbf{Z}_d e^{-Ls}\mathbf{x} + \mathbf{M}_d^{-1}\mathbf{Z}_d e^{-Ls}\mathbf{x}_m. \tag{44}$$

From Fig. 4, the last term is identical to $e^{-Ls}\mathbf{v}_{new}$. Thus, (28) and (36) is replaced with following modified relation:

$$\mathbf{v}_{new} = \mathbf{M}_d^{-1}[\mathbf{Z}_d\mathbf{x}_d - \mathbf{F}_e] - \mathbf{M}_d^{-1}\mathbf{Z}_d e^{-Ls}\mathbf{x} + e^{-Ls}\mathbf{v}_{new}. \tag{45}$$

IV. Simulation

A. Simulation Condition

A 2-DOF robot model is used (Fig. 5). For link 1 and 2, the lengths are l_1=35cm and l_2=29.4cm, the masses m_1=11.17kg and m_2=6.82kg, respectively [14], [15]. Coulomb (c_1=2.0N, c_2=3.08N) and viscous friction (b_1=b_2= 0.614N·s/rad) are included. The sampling time L is 1ms. A simple task, which involves contact with stiff plate (K_e=1.5×10^{5}N/m), is considered. The trajectory, the dashed line in Fig.5, is shown in Fig. 6.

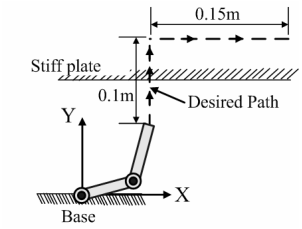

Fig. 5. 2 DOF SCARA Type Robot Schematic diagram

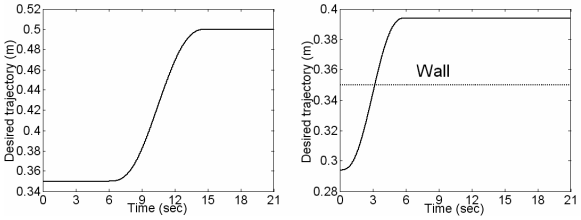

(a) *x* direction desired trajectory (b) *y* direction desired trajectory

Fig.6. Desired trajectory. Dotted line indicates the wall.

TABLE 1

POSITION RESPONSE OF EACH CONTROL

Control	DB-IC	IM-IC	PB-IC	Proposed control
Max.deviation (*mm*)	56.04	55.97	0.6	0.02

To verify the accuracy, the impedance error $\boldsymbol{\sigma} \in \Re^n$, defined as below, is considered.

$$\boldsymbol{\sigma}_{(t)} \triangleq \mathbf{M}_d(\ddot{\mathbf{x}}_{d(t)} - \ddot{\mathbf{x}}_{(t)}) + \mathbf{B}_d(\dot{\mathbf{x}}_{d(t)} - \dot{\mathbf{x}}_{(t)}) + \mathbf{K}_d(\mathbf{x}_{d(t)} - \mathbf{x}_{(t)}) - \mathbf{F}_{e(t)}. \quad (46)$$

If $\boldsymbol{\sigma}_{(t)}$ is zero vector, then (46) is the desired impedance dynamics in (1).

Two simulations were performed: First, to compare the accuracy and robustness of four control laws, control gains of each control were tuned to minimize $\boldsymbol{\sigma}$ under 10% modeling error (i.e. $\hat{m}_1$ =10.05kg, $\hat{m}_2$ =6.14kg was used for (5)). Simulation was then performed with unknown payload (6kg) at the end-effector side. Second, to confirm the accuracy of proposed control, four sets of desired impedance were implemented. Note that *no friction compensation* was used for all control laws in all simulations.

B. Comparison of Four Control Laws

Desired impedance parameters are designed as follows: $\mathbf{M}_d$=20**I** Kg, $\mathbf{B}_d$=900**I** N·s/m, $\mathbf{K}_d$=400**I** N/m. Note that $\mathbf{M}_d$ is physically constrained by the mass of robot [19]. With the aim of small contact force, small $\mathbf{K}_d$ is selected. Because the environment is stiff and has no damping, large $\mathbf{B}_d$ was selected for smooth motion.

The *x*-*y* position responses are shown in Fig. 7. In free space, the proposed controller shows the smallest position deviation, whereas DB-IC presents the largest (Table 1). Note that PB-IC shows remarkably small position deviation compared with that of DB-IC. Strictly speaking, the task cannot be executed with DB-IC or IM-IC. The position deviation is too large. Thus, DB-IC and IM-IC are excluded from further comparison.

The *y* direction force response with a payload is shown in Fig.8. The proposed control shows a small impact force (60.2N) compared with that (75.6N) of PB-IC. Further,

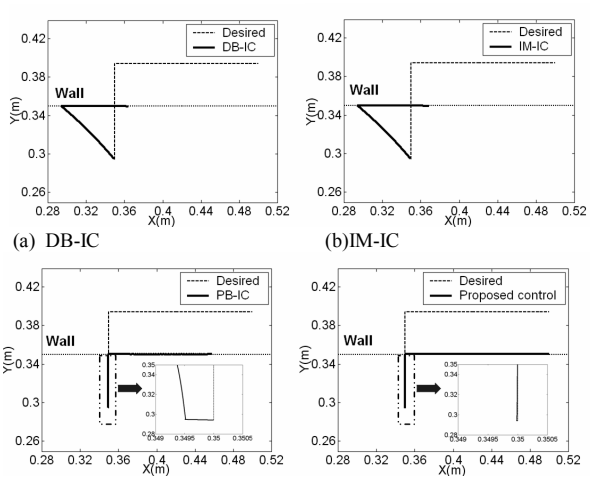

(a) DB-IC (b)IM-IC

(c) PB-IC (d) Proposed Impedance Control

Fig.7. Position responses with a payload. Dotted line indicates the wall.

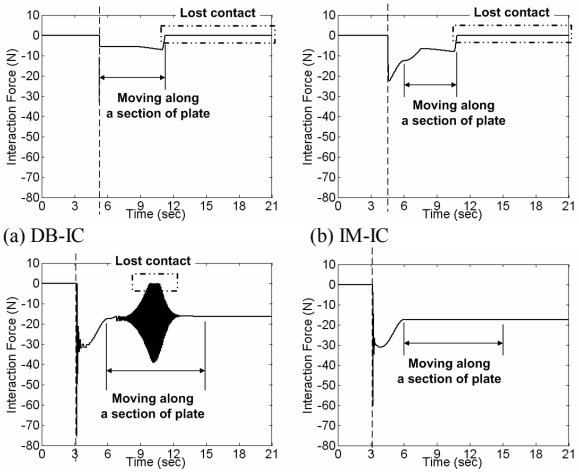

(a) DB-IC (b) IM-IC

(c) PB-IC (d) Proposed Impedance Control

Fig.8. Force responses with a payload. Dashed line indicates contact time

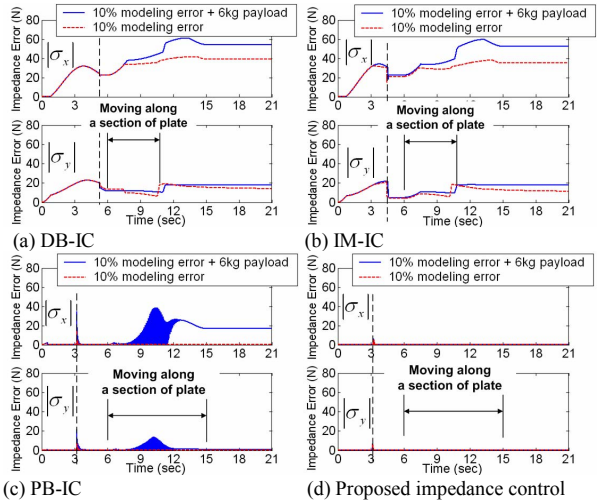

(a) DB-IC (b) IM-IC

(c) PB-IC (d) Proposed impedance control

Fig.9. Impedance errors. Dashed line indicates contact time

among the four control laws, only the proposed control does not lose contact with the environment while moving along a section of the plate from 6s to 15s. This indicates that the proposed control realizes desired impedance accurately due to the dynamics estimation error correction capability of the IMC structure.

The x and y direction absolute values of impedance error are shown in Fig. 9. Proposed control shows the smallest (and negligible) impedance error regardless of modeling error. DB-IC and IM-IC show large impedance error even without payload. Note that PB-IC shows remarkably small impedance error compared with those of DB-IC and IM-IC when 10% modeling error exists. However, with unknown payload, impedance error of PB-IC is increased significantly. It must be noted that proposed control does not use friction compensation at all. Further, as was mentioned, it does not use dynamics model. Note also that friction compensation may enhance the performance of DB-IC (and IM-IC) [4].

C. Desired Impedance Realization Performance

To verify the impedance realization accuracy of proposed control, four sets of desired impedance are implemented. The absolute impedance errors of four cases are shown in Fig. 10. Clearly, regardless of desired impedance, proposed control shows small impedance error.

V. Conclusion

In response to the "Accuracy/Robustness Dilemma in Impedance Control", both accurate and robust impedance control based on IMC is proposed. The suggested approach does not use dynamics computation or complex algorithm thanks to the IMC and TDE. In addition, robustness is enhanced without introducing the problematic inner loop dynamics. In other words, proposed control enhances robustness without sacrificing accuracy. It means that proposed control is free from the dilemma. Simulation results confirm that proposed control is robust against modeling error and accurate regardless of modeling error and desired impedance. Therefore, we believe that the proposed control is a simple yet effective solution to the "Accuracy /Robustness Dilemma in Impedance Control."

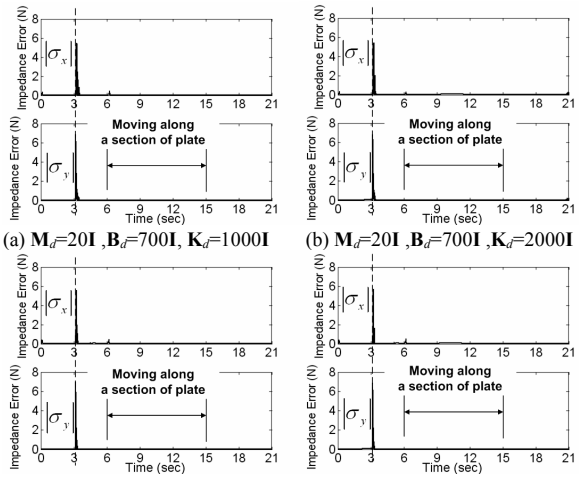

(a) $\mathbf{M}_d$=20**I** ,$\mathbf{B}_d$=700**I**, $\mathbf{K}_d$=1000**I** (b) $\mathbf{M}_d$=20**I** ,$\mathbf{B}_d$=700**I** ,$\mathbf{K}_d$=2000**I**

(c) $\mathbf{M}_d$=20**I**, $\mathbf{B}_d$=1200**I**, $\mathbf{K}_d$=1000**I** (d) $\mathbf{M}_d$=20**I**, $\mathbf{B}_d$=1200**I**, $\mathbf{K}_d$=2000**I**

Fig.10 Impedance error of proposed control under four different sets of desired impedance. Dashed line indicates contact time

References

[1] N. Hogan, "Impedance control: an approach to manipulation," *ASME J.of Dyn., Sys. Meas., and Contr.*, vol. 107, pp. 1–24, Mar. 1985.

[2] T. Valency, and M. Zacksenhouse, "Accuracy/robustness dilemma in impedance control," *ASME J. of Dyn., Sys. Meas., and Contr.*, vol. 125, pp.310-319, Sept. 2003.

[3] T. Yoshikawa, "Force control of robot manipulators," *in Proc. IEEE Intl. Conf. on Robotics and Automation*, San Francisco, CA, 2000, pp.220-226.

[4] S. Chiaverini, B. Siciliano, and L. Villani, "A survey of robot interaction control schemes with experimental comparison," *IEEE Trans. Mechatronics*, vol. 4, pp.273-285, Sept. 1999.

[5] D. A. Lawrence, "Impedance control stability properties in common implementations," *in Proc. IEEE Intl. Conf. on Robotics and Automation*, Philadelphia, PA, 1988, pp. 1185-1190.

[6] M. Vukobratović, and A. Tuneski, "Contact control concepts in manipulation robotics-an overview," *IEEE Trans.Ind. Electron.*, vol. 41, pp. 12- 24, Feb. 1994.

[7] J. De Shutter, H. Bruyninckx, W.-H. Zhu, and M. W. Spong, "Force control: a bird's eye view," *in Control Problems in Robotics and Automation: Future Directions*. San Diego, CA: Springer-Verlag, 1997, pp.1–17.

[8] F. Caccavale, C. Natale, B. Siciliano, and L. Villani, "Integration for the next generation: embedding force control into industrial robots," *IEEE Robot. Autom. Mag.*, vol. 12, pp. 53-64, Sep. 2005.

[9] S. P. Chan, and H. P. Chen, "Robust implementation of generalized impedance control for robot manipulators," *Advanced Robotics*, vol. 15, pp. 641-661, 2001.

[10] M.-C. Chien, and A.-C. Huang, "Adaptive impedance control of robot manipulators based on function approximation technique," *Robotica*, vol. 22, pp. 395-403, 2004.

[11] C.-C. Cheah, and D. Wang, "Learning impedance control for robot manipulators," *IEEE Trans. Robot. Autom.*, vol. 14, pp. 452-465, June 1998.

[12] C. G. Economou, and M. Morari, "Internal model control. 1. A unifying review and some new results," *Ind. Eng. Chem. Process Des. Dev.*, vol. 21, no.2, pp. 308–323, July 1982.

[13] K. Youcef-toumi and S.-T. Wu, "Input/Output linearization using time delay control," *ASME, J. of Dyn, Sys., Meas., Contr*, vol.114, pp10-19, 1992.

[14] P. H. Chang, J. W. Lee, and S. H. Park, "Time delay observer: a robust observer for nonlinear plants," *ASME J. Dyn., Sys. Meas., Contr.*, vol. 119, pp. 521–527, Sept. 1997.

[15] P. H. Chang, D. S. Kim, and K. C. Park "Robust force/position control of a robot manipulator using time-delay control," *Control Eng. Pract.*, vol. 3, 1995, pp. 1255-1264.

[16] P. H. Chang, B. S. Park, and K. C. Park "An experimental study on improving hybrid position/force control of a robot using time delay control," *Mechatronics*, vol. 6, 1996, pp. 915-931.

[17] O. Khatib, "A unified approach for motion and force control of robot manipulators: the operational space formulation," *IEEE Trans. Robot. Autom.*, vol. RA-3, pp. 43–53, Feb. 1987.

[18] S. Dasgupta, and Y. F. Huang, "Asymptotically convergent modified recursive least-squares with data-dependent updating and forgetting factor for systems with bounded noise," *IEEE Trans. Inf. Theory*, vol.IT-33, no. 3, pp. 383–392, May 1987.

[19] W. S. Newman, "Stability and performance limits of interaction controllers," *ASME, J. of Dyn. Sys., Meas., Contr.*, vol.114, pp.563-570, 1992.